



Effect of Minor Er on Microstructure and Mechanical Properties of AA6061 Alloy

Li Can, Chen Wen Lin* and Lei Yuan

School of Material Science and Engineering, Hefei University of Technology, China

Abstract

AA6061 alloys with different content of erbium were prepared by ingot-metallurgy method. The influences of erbium (Er) on the microstructure and mechanical properties of AA6061 alloy were investigated by optical microscopy (OM), scanning electron microscopy (SEM) with energy dispersive spectrometer (EDS), transmission electron microscopy (TEM) and X-ray diffraction (XRD) analysis. It has been found that addition of about 0.3wt.% Er can achieve the most effective grains size refinement for the as-cast alloy, and primary AlMgSiCuEr phase is observed in the α -Al grains. After solid solution treatment at 565 °C for 30 min, water quenched and finally aged at 200 °C for 6h, the ultimate tensile strength (330 MPa) elongation (24.4%) of the alloy with 0.3 wt.% Er are higher than that of the Er-free alloy. The relationship between the yield strength and grain size correlates well with Hall-Petch equation. The secondary Al₃Er precipitates with a stable L1₂ structure not only pin the movement of dislocation but also generate strong grain refinement in the aged alloy which obtain fine equiaxed grains. Compared with AA6061 alloy, the alloy with 0.3 wt.% Er additions has numerous equiaxed dimples uniformly distributed on the fracture surface. It indicates that the fracture characteristics exhibit typical ductile fracture.

Keywords

AA6061 alloy, Erbium, Microstructure, Mechanical property

Introduction

6xxx series aluminum alloys containing Mg and Si as major addition elements show a high strength-to-density ratio, a good electrical conductivity ability and a superior corrosion resistance, which are widely applied to the areas of fuel-efficient cars and high-speed trains as lightweight structural materials [1]. AA6061 aluminum alloy has excellent weldability and corrosion resistance but compared with AA6013, AA6069 aluminum alloy, its strength is lower, which limits its application on the automobile body sheets and the door frame which required higher strength and stiffness. Therefore, minor-alloying, addition of small amount of alloying elements to the based alloy is used as an effective method to increase the strength of the traditional AA6061 alloys. It has important significance for its application in the industry of car manufacturing.

It is well accepted that small additions of rare earth elements are of great importance to improve the mechanical properties of aluminum alloys and provide extended alloying capabilities [2]. A previous work revealed that, with the addition of 0.15% rare earth Sc, the mechanical

properties of AA7085 aluminum alloy are improved significantly, and the denudation level is improved from E_B to P_B [3]. However, the applications of Sc containing alloys are extremely restricted due to the high cost of Sc addition. Instead, much attention was focused on rare earth Erbium (Er), which is much cheaper than Sc. In a recent study, adding 0.3% Er into Al-Mg-Si-Cu alloy its tensile strength and elongation are increased by 7% and 4% respectively, at the same time its recrystallization temperature range is increased by 40 °C [4]. Besides, it has been reported that Er can refine the grains size of the as-cast Al-Mg-Mn-Zr alloy [5]. It's found that the inter- and intragranular primary Al₃Er (L1₂) precipitates are formed, and the Er-containing alloy has finer grains, owing to the

***Corresponding author:** Chen Wen Lin, School of Materials Science and Engineering, Hefei University of Technology, Hefei 230009, P.R.China, Tel: 0551-62904578

Accepted: August 13, 2018; **Published online:** August 15, 2018

Citation: Can L, Lin CW, Yuan L (2018) Effect of Minor Er on Microstructure and Mechanical Properties of AA6061 Alloy. Adv Metallurg Mater Eng 1(1):8-14

intergranular Al_3Er precipitates that inhibit grain growth [6]. The Al_3Er particles can precipitate from the matrix during homogenization and solution of the aluminum alloy, which not only pin dislocation and grain boundary, but also increase the mechanical properties and the weldability of the aluminum alloys [7]. Some researchers also found that trace Er can significantly refine alloy dendritic structure and improve the thermal stability of alloy [8]. Furthermore, the paper [9] finds the Er modified the eutectic structure from a coarse plate-like and acicular structure to a fine branched and fibrous one. At present, rare earth Er microalloying has become an important direction to improve the comprehensive performance of aluminum alloy. Currently, research about the effect of Er on aluminum alloy mostly focus on 5xxx and 7xxx alloys, but less on the 6xxx aluminum alloy.

In the present research, Er was added to an experimental AA6061 aluminum alloy. The effect of Er on the microstructures and the mechanical properties of AA6061 alloy was studied, so as to improve its mechanical properties and provide reference for the study of the 6xxx aluminum alloys containing Er.

Experimental Procedure

Four kinds of alloys with different Er content were prepared in laboratory and the detailed main chemical compositions are listed in Table 1. Commercial pure alu-

minum (ingot, > 99.99% purity) 99.5% purity Mg and master alloys Al-20Si (wt.%), Al-50Cu (wt.%), Al-20Mn (wt.%) as well as Al-9.92Er (wt.%) were used to prepare the testing alloys. The melting process was carried out in graphite crucible resistance furnace and the alloy was poured into water-cooled copper mould as ingot at 700 °C with the size of 100 mm × 50 mm × 20 mm.

After homogenization heat treatment at 555 °C for 10h, the oxide scale of ingot was removed, then hot-rolled and cold-rolled to 1 mm-thick sheet, which corresponds to 87.5% total reduction. For the hot rolling process, each 8 mm-thick specimen was preheated to 430 °C, and rolled to 4 mm with a reduction ratio of 50%. The hot rolled specimens were then annealed to release existing stress and were finally cold rolled to a final thickness of 1 mm with a reduction ratio of 75%. The rolled specimens were heated at 565 °C for 30 min, water quenched and finally aged at 200 °C for 6h in the heat-treating furnace model KSL-1700X (i.e. T6 heat treating). The quenching transfer time is less than 15s, and the water temperature

Table 1: Chemical composition of experimental alloys (wt.%).

Alloy No.	Mg	Si	Cu	Mn	Er	Al
1 #	1.09	0.64	0.31	0.14	0	Balance
2 #	1.10	0.66	0.30	0.15	0.19	Balance
3 #	1.11	0.65	0.30	0.14	0.31	Balance
4 #	1.08	0.66	0.29	0.16	0.40	Balance

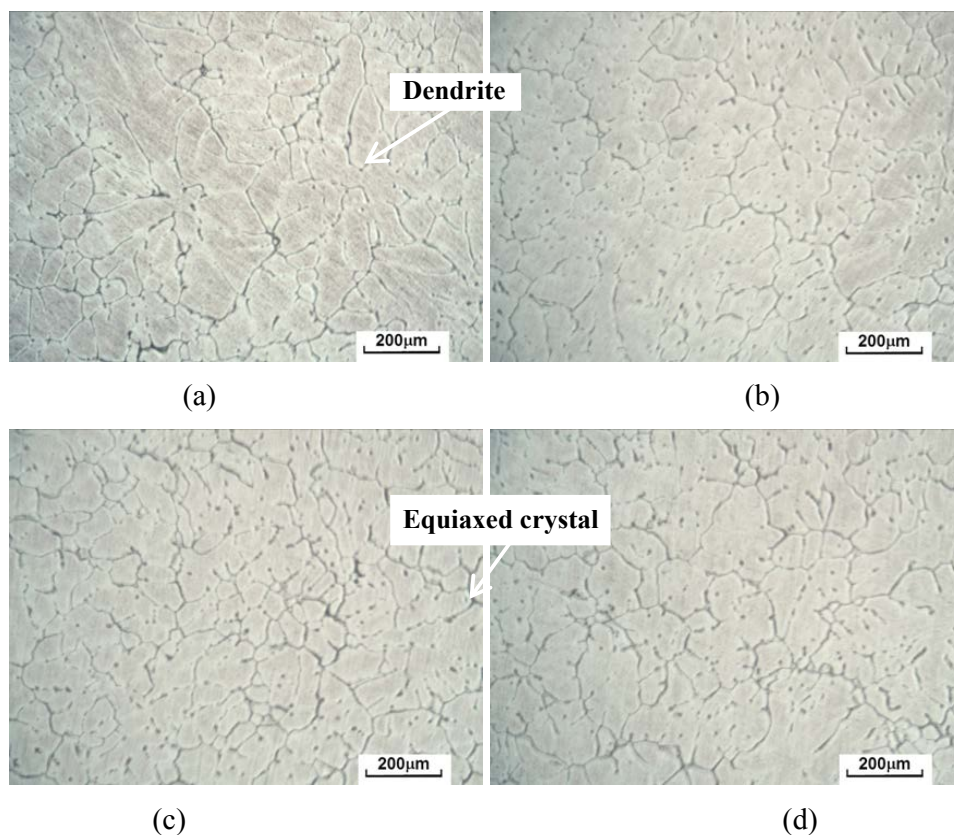


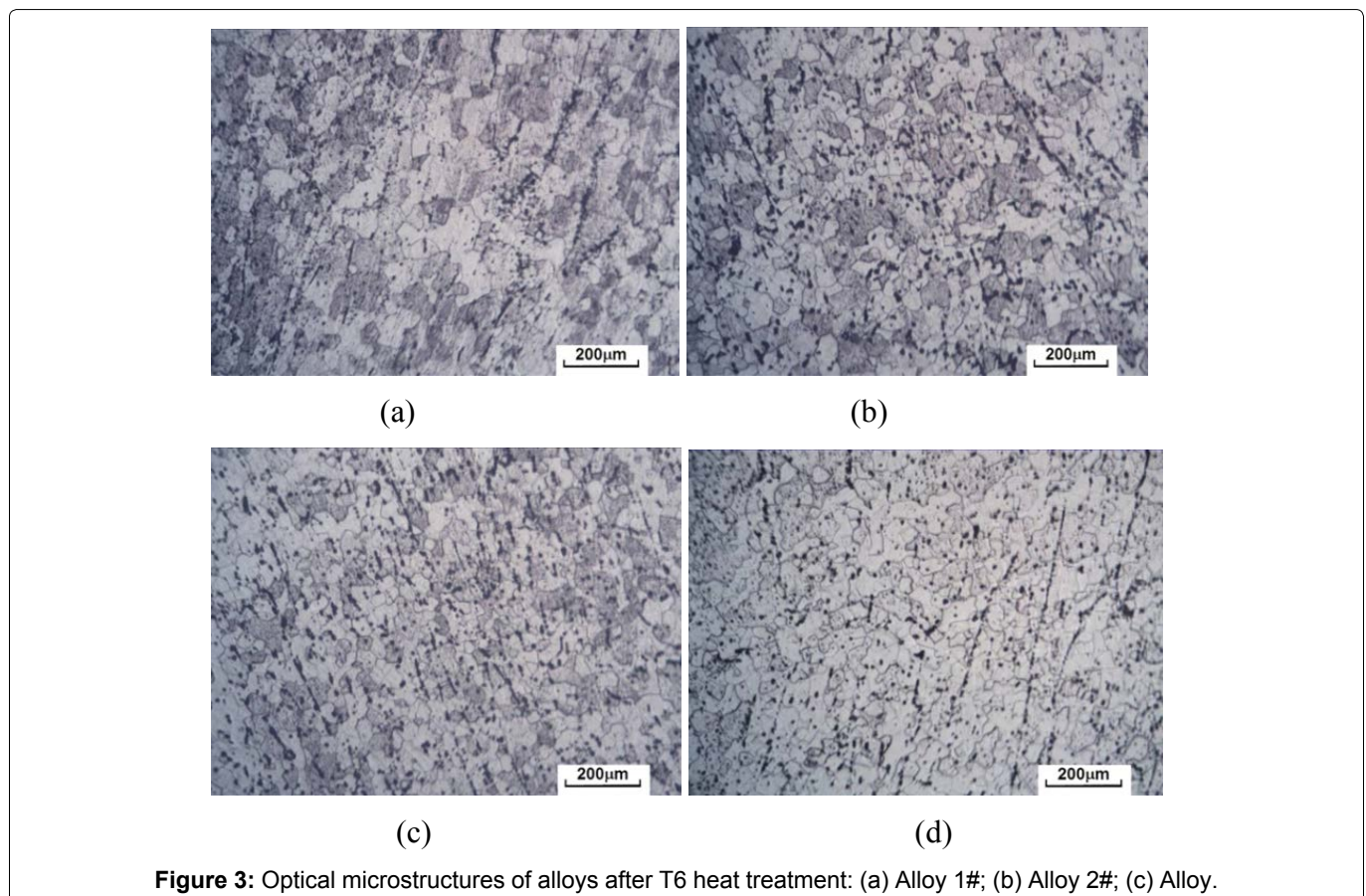
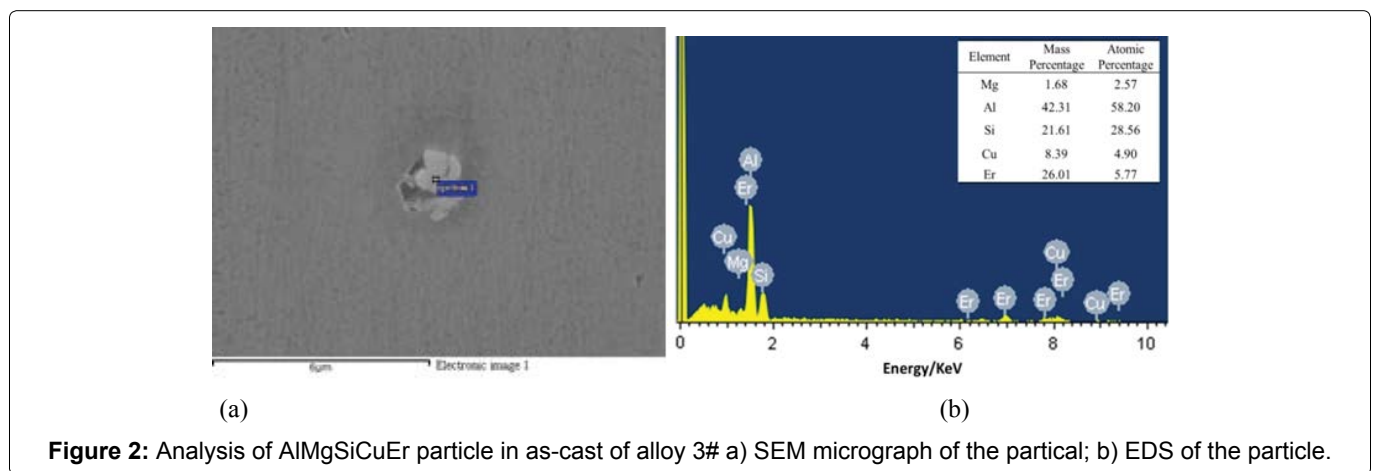
Figure 1: Optical microstructures of as-cast alloys: (a) Alloy 1#; (b) Alloy 2#; (c) Alloy 3#; (d) Alloy 4#.

is below 25 °C. Metallographic samples of as-cast and T6 treated alloys were prepared by standard mechanical polishing and then etched with 0.5% HF. Microstructure of the etched samples were observed and analyzed by means of the optical microscope model MR5000. Tensile test was carried out on SANS-100KN micro-controlled electronic universal testing machine. The tensile speed was 1 mm.min⁻¹, and the average value of 3 samples was determined in each state. The microstructure and fracture morphology of the alloy was characterized by SU8020 field emission scanning electron microscope and JEM-2100FX type field emission transmission electron microscope.

Results and Discussion

Microstructure

Figure 1 depicts the optical micrographs of the as-cast alloys with different Er concentration. All the samples show a mixed morphology of dendrite and equiaxed crystal. It can be clearly observed that dendrite spacing is larger and the grain size is not uniform in the alloy 1# without addition of Er element, but the quantity of grain boundaries increases and some dendrites begin to refine with the increase of Er content. When the Er content reaches 0.3wt.% (Figure 1c), dendrite spacing significantly decreased and the grain size is relatively fine



and uniform. Further increase of Er content to 0.4 wt.% only leads to less obvious change in grain size.

During the solidification in casting, Er has low solubility in the α -Al and accumulate at the front of interface between solid and liquid, which causes composition undercooling, to make the straight interface disturbed and become unstable in the growth process, retard the advancing speed of solid-liquid interface to some extent. It allows the remaining liquid has more time to nucleate again, which reduces dendrite spacing and result in the grain refinement [10,11]. Except for the grain structure, also the phase composition of the alloys needs to be identified. Figure 2 shows the SEM image of the precipitation and EDS results of the as-cast alloy 3#. The precipitated phase contains five elements, which are Al, Mg, Si, Cu, Er respectively and identified as Er-containing intermetallics. Equiaxed grains appear in the grain structure because nucleus relatively limited growing time which provide resistance to develop dendrite in the alloy. It's consistent with the research results of Bai, et al. [12].

Figure 3 shows the microstructure of experimental alloys after the rolling deformation and T6 heat treatment. It can be seen that after heat treatment, uniform equiaxed recrystallized grains are formed in alloys. Based on the linear intercept method, the average grain size of the four alloys are 90 μm , 69 μm , 40 μm , 45 μm respectively. The standard deviation errors are 9 μm , 7 μm , 6 μm , 6 μm respectively. It's well known that the grain size has a very important influence on the properties of the material. Fine grains can improve the strength and plasticity of the material [13]. On the one hand, the increase of grain boundary enlarges the resistance of dislocation slip and improves the strength of the alloy. On the other hand, the greater the number of grains in unit volume, the same amount of deformation can be dispersed into

more grains, resulting in uniform deformation without causing excessive local stress concentration, leading to premature generation and development of cracks.

Figure 4 shows the XRD results of No.1 and No.3 alloys after T6 heat treatment. It can be seen that after solid solution and aging treatment, Mg_2Si phase, Al_2Cu phase, AlMnSi phase are present in both kinds of alloys, and Al_3Er phase is detected in the No.3 alloy. The results were consistent with the presence form of the Er in the Al-Zn-Mg alloy and Al-Mg alloy [14,15]. The interface energy between Al_3Er and the matrix is very low and is very stable owing to the similarity between the crystal lattices of the aluminum matrix and the Al_3Er phase in terms of their structure and dimension. Al_3Er exhibits a stable L1_2 structure in α -Al matrix and has a small lattice parameter misfit 4.1% with the aluminum matrix. Besides, it can strongly inhibit recrystallization and prevent grain growth of the aluminum alloy [16]. These particles will prohibit the movement of grain boundaries. Dislocations are strongly pinned and grain boundaries can hardly pass the particles [6,17].

Mechanical properties

The tensile true stress-strain curves of experimental alloys in the T6 state and the specific results are given in (Figure 5 and Table 2). The results indicates the positive effect of Er content on the strength (UTS and YS) and plasticity. Comparing with the unmodified alloy, the tensile properties of Er modified alloys are superior, and the mechanical properties of the alloy achieve the best when the Er content is 0.3wt.%. The ultimate tensile strength, yield strength and elongation of the alloy 3# were increased by 38 MPa, 26 MPa and 4.3%, respectively, than those of alloy 1#. In combination with Figure 3 and Figure 4, the Er-containing precipitates and finer grains lead

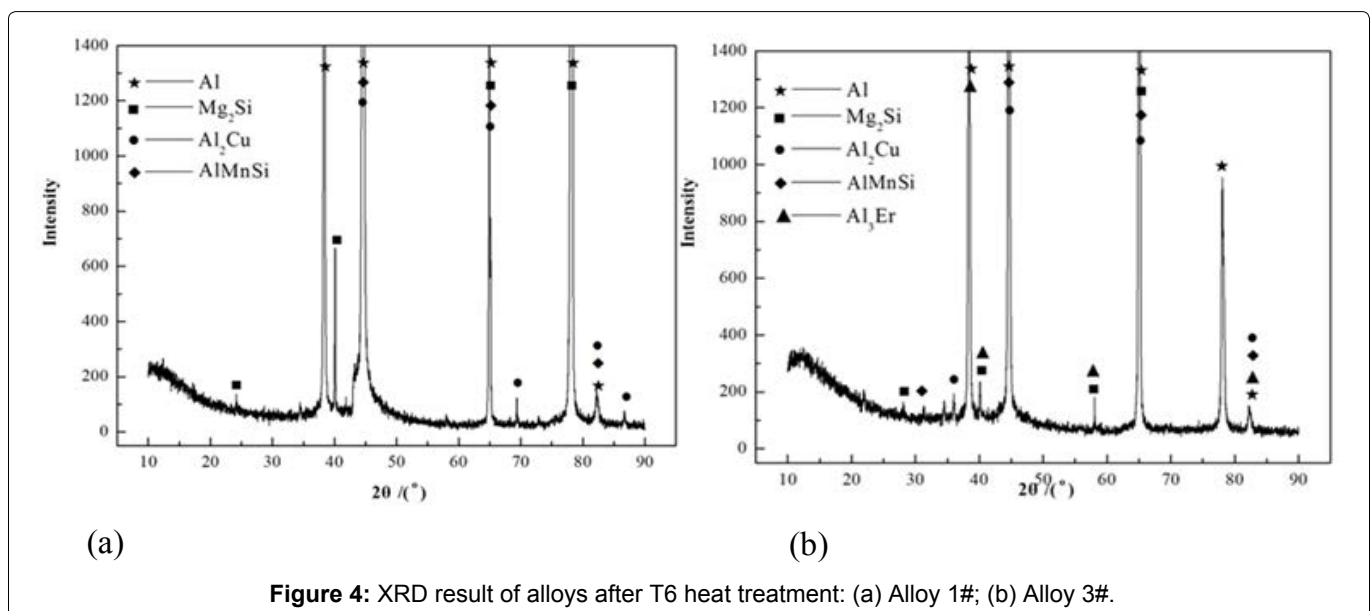


Figure 4: XRD result of alloys after T6 heat treatment: (a) Alloy 1#; (b) Alloy 3#.

Table 2: Mechanical properties of T6 alloys.

Alloy No.	Er content, w/%	UTS/MPa	YS/MPa	Elongation/%	Hardness/HB	standard deviation
1 #	0	292	230	20.11	84.6	4.43
2 #	0.19	303	241	21.30	89.7	2.31
3 #	0.31	330	256	24.43	103.2	4.55
4 #	0.40	325	252	23.31	94.7	3.74

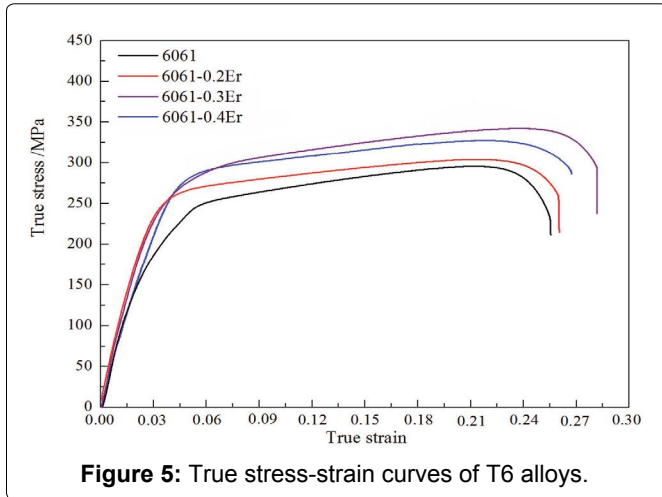


Figure 5: True stress-strain curves of T6 alloys.

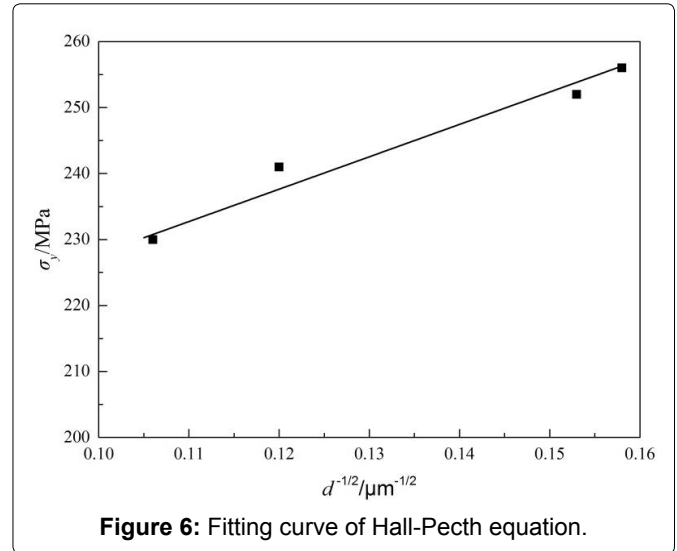


Figure 6: Fitting curve of Hall-Petch equation.

to the increase in elongation and hardness. Obviously, an addition of 0.3wt.% Er can improve the comprehensive properties of alloys. From the experimental results, one can also find the decrease in strength of alloy 4#. It can be deduced that the Al_3Er precipitates become larger, which is the result of segregation of Er atom at the grain boundary.

Combining Figure 3 with mechanical properties of alloys, the relationship between grain size and yield strength can be explained by Hall-Petch relation:

$$\sigma_y = \sigma_0 + Kd^{-1/2}$$

In the formula, σ_y is the yield strength; σ_0 is the yield strength of single crystal; K is the slope of Petch; d is the diameter of the grain. It can be seen from the formula, the yield strength of the material increases with the decrease of grain size. The smaller the grain size of the material, the higher the yield strength. This is mainly because dislocation slip is hindered by grain boundary, and the number of grain boundaries directly depends on the size of grain. Therefore, the smaller the grain size, the more the grain boundary in the unit volume, which increase the resistance of dislocation slip and the yield strength [18]. (Figure 6) is the Hall-Petch curve based on the grain size and yield strength of the alloys with different Er content, and the Hall-Petch formula is $\sigma_y = 179 + 491d^{-1/2}$.

Artificial aging leads to precipitation of various phases (leading to the stable β phase) and the matrix was heavily strained. It is well known that precipitation hardening is a procedure that enhances the mechanical properties of aluminium alloys by arrangement and pre-

cipitation of scattered second particles inside the metal matrix [19]. The precipitation sequence has been studied by several groups [20,21]. The hardness and strength are determined by the precipitate type, density and size [22]. Figure 7 shows TEM micrographs of alloy 3# in the rolling state and T6 state. It can be seen that the alloy exhibits a high-density dislocation tangling state after rolling. The dislocation density of the alloy decreased relatively and a large number of dislocations occurred around the precipitates (as point B in Figure 7b) and tangled up in a messy way to form dislocation pile-up (as point A in Figure 7b) after the aging treatment. From the Figure 7c, it can be seen that some dislocations form dislocation walls and subgrains. These precipitates are pinning around the dislocation wall and subgrain boundaries, hindering dislocation movement and subgrain growth. When the moving dislocations meet these particles, they may form dislocation loops around the particles or bypass the solute atoms in a way of cutting particles, which further improve the strengthening effect of alloy [23,24]. At the same time, it can be seen from the local enlarged view in Figure 7d that the formation of Al_3Er phase precipitates in the alloy has strong pinning effect on dislocations. Owing to these particles, the mechanical properties of alloy is improved significantly. To summarize, this can attribute to the fine grain strengthening, precipitation strengthening, and substructure strengthening, which have a comprehensive enhancing effect on mechanical properties.

The SEM micrographs of the fracture surface of No.1

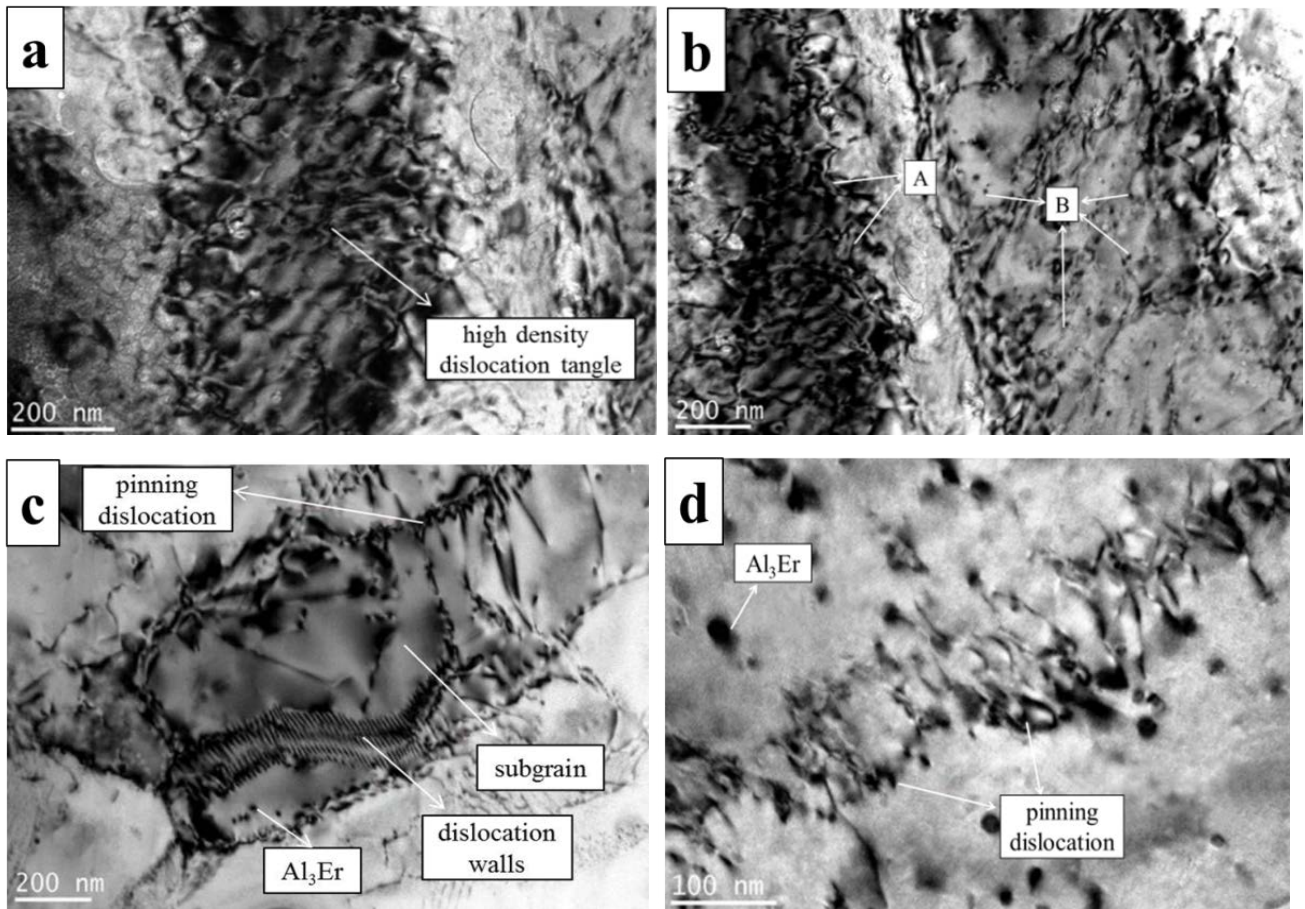


Figure 7: TEM micrographs of T6 alloy 3#; (a) Rolled-state; (b,c) Bright field TEM micrograph; (d) Local enlarged view.

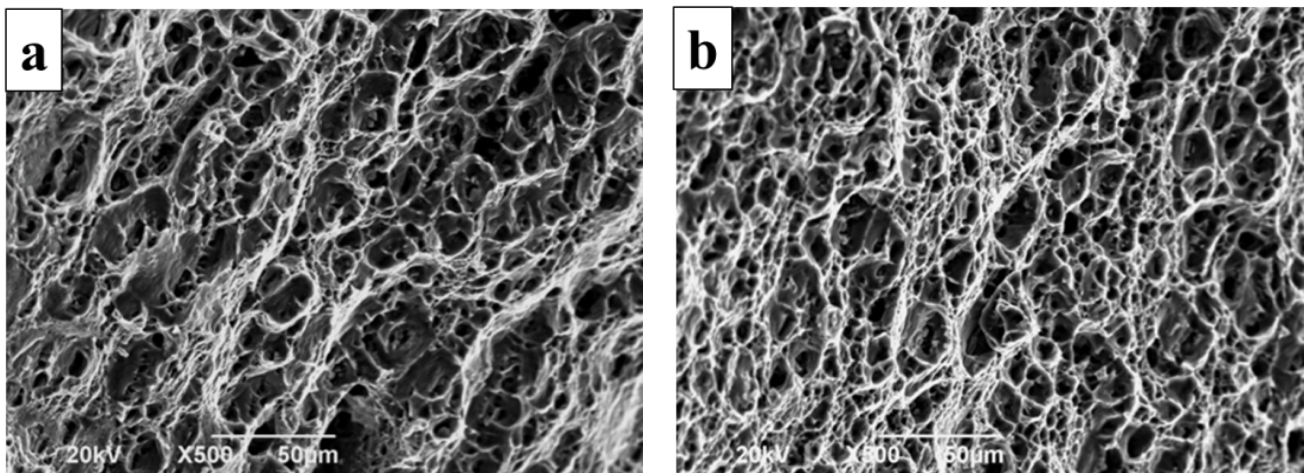


Figure 8: SEM micrographs of the fracture surface; (a) Alloy 1#; (b) Alloy 3#.

and No.3 alloys in the T6 treated condition are illustrated in Figure 8. Fracture morphology can be a very good characterization of the plasticity. As can be seen in Figure 8b, the morphology of dimple fracture from AA6061 alloy modified with 0.3 wt.% Er is obvious, and the dimple is very deep and well-distributed, so the fracture morphology is characteristic of ductile fracture. And it results in higher mechanical properties of alloys. The dimples of

unmodified No. 1 alloy are less and uneven distributed. Therefore, their mechanical properties are less than that of modified alloys. It is shown that the addition of Er leads to a significant increase in the plasticity of the alloy, which is consistent with the data in Table 2. The ductility of No.3 alloy improves which is related mainly with the beneficial behavior of rare earth elements during casting and solidifying [25,26].

Conclusion

Addition of rare earth element Er into AA6061 aluminum alloy can form the composite AlMgSiCuEr phase which be used as a heterogeneous nucleation core to refine the as-cast grains during the process of solidification.

After T6 treatment, the mechanical properties of alloy are obviously improved, and the strengthening of alloy is mainly the result of the combination of precipitation strengthening, fine grain strengthening and substructure strengthening. The yield strength of the alloy increases with the decrease of grain size, the relationship between the yield strength and grain size correlates well with Hall-Petch equation. The Hall-Petch formula is $\sigma_y = 179 + 491d^{-1/2}$.

When the content of Er is 0.3wt.%, the tensile strength, yield strength and elongation of the alloy reach the optimum. The number of dimples in the alloy fracture increases remarkably, and the distribution is uniform. The plasticity of the alloy is remarkably improved.

References

1. Yuan W, Liang Z, Zhang C, et al. (2012) Effects of La addition on the mechanical properties and thermal-resistant properties of Al-Mg-Si-Zr alloys based on AA 6201. *Materials & Design* 34: 788-792.
2. Hu X, Jiang F, Ai F, et al. (2012) Effects of rare earth Er additions on microstructure development and mechanical properties of die-cast ADC 12 aluminum alloy. *Journal of Alloys & Compounds* 538: 21-27.
3. Gao Yan, Chen Wen lin (2015) Effect of rare earth on strength and corrosion properties of 7085 aluminum alloy. *Transactions of Materials and Heat Treatment* 36: 126-132.
4. WU Yue, Chen Wen lin, LI Wei (2014) Effect of solution treatment on Microstructure and mechanical properties of Al-0.9Mg-0.6Si-0.7Cu alloy. *Transactions of Materials and Heat Treatment*.
5. Wen S P, Xing Z B, Huang H, et al. (2009) The effect of erbium on the microstructure and mechanical properties of Al-Mg-Mn-Zr alloy. *Materials Science & Engineering: A* 516: 42-49.
6. Booth Morrison C, Seidman DN, Dunand DC (2012) Effect of Er additions on ambient and high-temperature strength of precipitation-strengthened Al-Zr-Sc-Si alloys. *Acta Materialia* 60: 3643-3654.
7. WEN Shen ping (2011) Research progress of Er-containing aluminum alloy. *The Chinese Journal of Nonferrous Metals* 21: 61-63.
8. Wanhui Zhao, Shengping Wen, Wei Wang, et al. (2014) Effects of Er and Zr additions on precipitation and recrystallization of Al-Mg alloy. *International Conference on Computer Science and Electronic Technology*.
9. Kord S, Alipour M, Siadati M H, et al. (2018) Effects of Rare Earth Er Additions on Microstructure and Mechanical Properties of an Al-Zn-Mg-Cu Alloy. *TMS Meeting & Exhibition* 441-449.
10. XU Guo fu, YANG Jun jun, JIN Tou nan, et al. (2006) Effects of trace rare-earth element Er on microstructure and properties of Al-5Mg alloy. *The Chinese Journal of Nonferrous Metals*.
11. YANG Fu bao (2008) Effect of Er on the microstructure and mechanical properties of as-cast Al-Mg-Mn-Zn-Sc-Zr-(Ti) filler metals. *Acta Metall Sin* 44: 911-916.
12. Bai S, Liu Z, Li Y, et al. (2010) Microstructures and fatigue fracture behavior of an Al-Cu-Mg-Ag alloy with addition of rare earth Er. *Materials Science & Engineering A* 527: 1806-1814.
13. Mondolfo LF (2016) Grain Refinement in Aluminum Alloys. *Essential Readings in Light Metals*. Springer International Publishing.
14. Fang H C, Chao H, Chen K H (2014) Effect of Zr, Er and Cr additions on microstructures and properties of Al-Zn-Mg-Cu alloys. *Materials Science & Engineering: A* 610: 10-16.
15. Yang D, Li X, He D, et al. (2013) Effect of minor Er and Zr on microstructure and mechanical properties of Al-Mg-Mn alloy (5083) welded joints. *Materials Science & Engineering: A* 561: 226-231.
16. Li H, Gao Z, Yin H, et al. (2013) Effects of Er and Zr additions on precipitation and recrystallization of pure aluminum. *Scripta Materialia* 68: 59-62.
17. Wen S P, Gao K Y, Li Y, et al. (2011) Synergetic effect of Er and Zr on the precipitation hardening of Al-Er-Zr alloy. *Scripta Materialia* 65: 592-595.
18. Loucif A, Figueiredo RB, Baudin T, et al. (2012) Ultrafine grains and the Hall-Petch relationship in an Al-Mg-Si alloy processed by high-pressure torsion. *Materials Science & Engineering: A* 532: 139-145.
19. Abúndez A, Pereyra I, Campillo B, et al. (2016) Improvement of ultimate tensile strength by artificial ageing and retrogression treatment of aluminium alloy 6061. *Materials Science & Engineering: A* 668: 201-207.
20. Marioara CD, Nordmark H, Andersen SJ, et al. (2006) Post- β phases and their influence on microstructure and hardness in 6xxx Al-Mg-Si alloys. *J Mater Sci* 41: 471-478.
21. Yassar SR, Field PD, H Weiland (2005) Transmission electron microscopy and differential scanning calorimetry studies on the precipitation sequence in an Al-Mg-Si alloy: AA6022. *J Mater Res* 20: 2705-2711.
22. Buha J, Lumley RN, Crosky AG, et al. (2007) Secondary precipitation in an Al-Mg-Si-Cu alloy. *Acta Mater* 55: 3015-3024.
23. WU Yue, CHEN Wen lin, LI Wei, et al. (2015) Effect of microalloying of Sc on microstructure and properties of Al-Mg-Si-Cu alloys. *Journal of Plasticity Engineering* 22: 70-75.
24. Maisonnelle D, Suery M, Nelias D, et al. (2011) Effects of heat treatments on the microstructure and mechanical properties of a 6061 aluminium alloy. *Materials Science & Engineering: A* 528: 2718-2724.
25. Hosseinifar Mehdi, Malakhov Dmitri V (2008) Effect of Ce and La on microstructure and properties of a 6XXX series type aluminum alloy. *J Mater Sci* 43: 7157-7164.
26. Wang Shaohong, Zhou Heping, Kang Yuping (2003) The influence of rare earth elements on microstructures and properties of 6061 aluminum alloy vacuum-brazed joints. *J Alloys Compd* 352: 79-83.